

## Unexpected photoactivation pathways in a folate-receptor-targeted *trans*-diazido Pt(IV) anticancer pro-drug.

Albert Gandioso,<sup>a</sup> Anna Rovira,<sup>a</sup> Huayun Shi,<sup>b</sup> Peter J. Sadler,<sup>b</sup> and Vicente Marchán<sup>\*a</sup>

<sup>a</sup>Departament de Química Inorgànica i Orgànica, Secció de Química Orgànica, IBUB, Universitat de Barcelona, Martí i Franquès 1-11, E-08028 Barcelona (Spain).

E-mail: [vmarchan@ub.edu](mailto:vmarchan@ub.edu)

<sup>b</sup>Department of Chemistry, University of Warwick, Coventry CV4 7AL, UK.

### Abstract

A conjugate between a photoactive *trans*-diazido Pt(IV) pro-drug, *trans,trans,trans*-[Pt(N<sub>3</sub>)<sub>2</sub>(OH)<sub>2</sub>(py)<sub>2</sub>], and folic acid has been synthesized and fully characterized by high resolution ESI-MS, NMR and UV-vis spectroscopy. Photoactivation of the Pt-folate conjugate with visible light confirmed the generation of cytotoxic Pt(II) species capable of binding to guanine nucleobases. Importantly, photoreduction of the Pt(IV) complex triggered the photodecomposition of the folate vector into a *p*-aminobenzoate-containing fragment and several pterin derivatives, including 6-formylpterin. Besides exhibiting high dark stability in physiological-like conditions, the Pt-folate conjugate was *ca.* 2x more photocytotoxic towards MCF-7 breast cancer cell line than its parent Pt(IV) complex with a high photoselectivity index (PI >6.9). The higher photocytotoxicity of the conjugate may be a consequence of its higher cellular accumulation and of the generation of a set of different cytotoxic species, including Pt(II) photoproducts and several pterin derivatives, which are known to generate ROS.

Folate receptors (FRs), which are involved in the uptake of folic acid (vitamin B9), exist in three different isoforms ( $\alpha$ ,  $\beta$ , and  $\gamma$ ). Among them, FR $\alpha$  is expressed at very low levels in normal tissues, but it is highly up-regulated on the cell surface of a wide variety of cancers, including ovarian, kidney, brain, triple-negative breast, colon, lung tumors and head and neck carcinomas, making it a well-established target for anticancer drug development.<sup>1</sup> Owing to the frequent overexpression of FR $\alpha$  on human cancers (~ 40%), the attachment of folate to potent cytotoxic agents represents a promising approach in tumor-targeted chemotherapy.<sup>2</sup> Indeed, folate-based small drug conjugates bind to FR $\alpha$  on cancer cells with high affinity resulting in subsequent internalization through receptor-mediated endocytosis, in a process usually as effective as that displayed by folic acid in its free form.

In recent years, a large variety of chemotherapeutic agents have been conjugated to folic acid for active targeted drug delivery, including small organic drugs such as chlorambucil,<sup>3</sup> paclitaxel and derivatives,<sup>4</sup> mitomycin C,<sup>5</sup> and photosensitizers for application in photodynamic therapy.<sup>6</sup> One of the most successful folate-small drug conjugates is Vintafolide, which delivers a microtubule-destabilizing drug to tumors that overexpress FR $\alpha$ .<sup>7</sup> Vintafolide has shown promising results, both as a single agent, as well as in combination with doxorubicin in different clinical trials, being Phase III trials completed in 2014 for the treatment of platinum-resistant ovarian cancer.

Although less deeply investigated, folate conjugates involving metal-based anticancer drugs<sup>8</sup> represent a viable choice for developing novel targeted chemotherapeutic agents operating with alternative mechanisms of action compared with organic drugs,<sup>9</sup> which would facilitate overcoming of inherent or acquired resistance in cancer cells. Among them, Pt(II) and Pt(IV) complexes have received great attention owing to the success history of cisplatin and its two FDA-approved analogues in the clinical treatment of cancer. One of the first examples of a folate-platinum conjugate was reported by Gibson and co-workers who developed long-circulating PEGylated carboplatin analogues with improved cell permeation abilities by conjugating the platinum moiety to folate-targeted PEG carriers.<sup>10</sup> Another interesting approach to delivering platinum drugs to cancer cells overexpressing FR $\alpha$  was described by Lippard and collaborators who took advantage of the two axial positions of Pt(IV) complexes to attach them simultaneously to folate and to a delivery system based on a single-wall carbon nanotube.<sup>11</sup>

Photoactivatable metallodrugs have also demonstrated great potential in photoactivated chemotherapy (PACT).<sup>12</sup> Diazidodihydroxido Pt(IV) pro-drugs, such as *trans,trans,trans*-[Pt(N<sub>3</sub>)<sub>2</sub>(OH)<sub>2</sub>(py)<sub>2</sub>] (1, Fig. 1), are particularly interesting for improved treatment of cancer due to their high stability, low toxicity in the dark, potent photocytotoxicity upon irradiation with visible light, and novel mechanisms of action.<sup>13</sup> In addition, derivatization of the two detachable axial ligands in Pt(IV) complexes offers the possibility to modulate or improve

their physicochemical and pharmacological properties such as aqueous solubility, cellular uptake and target specificity.<sup>14</sup> In this context, we have conjugated Pt(IV) pro-drug **1** to small peptides targeting different integrin receptors ( $\alpha_v\beta_3/\alpha_v\beta_5$  or  $\alpha_6$ ) that are overexpressed in various cancer cells.<sup>15</sup> Complex **1** has also been attached to drug delivery upconversion-luminescent nanoparticles,<sup>16</sup> hydrogels,<sup>17</sup> and block copolymer micelles<sup>18</sup> for triggering activation with longer wavelengths and improving selectivity.

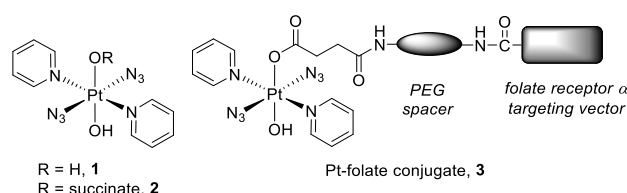
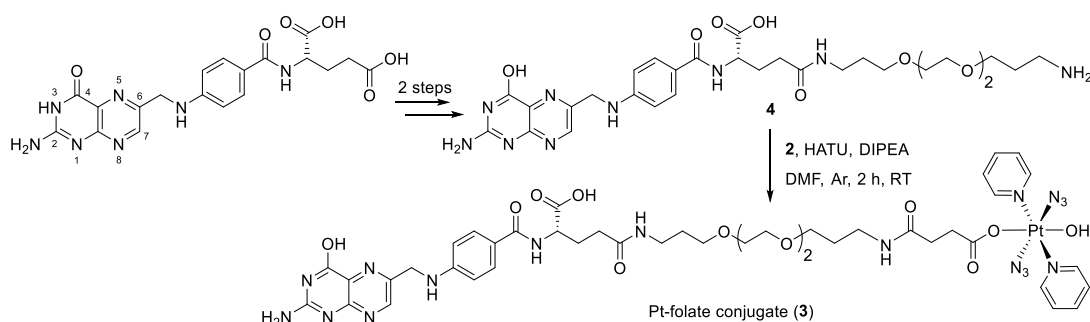


**Fig. 1** Structure of *trans,trans,trans*-[Pt(N<sub>3</sub>)<sub>2</sub>(OH)<sub>2</sub>(py)<sub>2</sub>] (**1**), *trans,trans,trans*-[Pt(N<sub>3</sub>)<sub>2</sub>(OH)(succ)(py)<sub>2</sub>] (**2**), and the schematic representation of the Pt–folate conjugate (**3**).

Based on these antecedents, herein we report the conjugation of Pt(IV) pro-drug **1** to folic acid via its monosuccinate derivative (**2**, Fig. 1), and investigation of the photoactivation, photocytotoxicity and cellular accumulation of the resulting Pt-folate conjugate (**3**). As previously found with conjugates involving photoactivatable metallodrugs and targeting vectors based on receptor-binding peptides,<sup>15,19</sup> the selectivity of the Pt-folate conjugate towards cancer cells is controlled at two levels. First, the conjugate will be internalized only in cancer cells overexpressing FR $\alpha$ , and second, the release of cytotoxic Pt(II) species from the Pt(IV) pro-drug will take place only at the tumor irradiation site. As shown in Fig. 1, a polyethylene glycol (PEG) spacer was introduced between the Pt(IV) complex and folate to increase hydrophilicity and biocompatibility, as well as to separate both moieties in the conjugate, the latter being an important issue to maintain recognition by FR $\alpha$ . Besides increasing water solubility, PEG spacers are known to minimize aggregation and non-specific uptake of the resulting conjugates by cells.<sup>7</sup> In addition, derivatization of folic acid through the  $\gamma$  carboxyl group is known not to alter significantly binding affinity for FR $\alpha$ , whereas the corresponding  $\alpha$ -carboxyl-linked conjugates are not readily recognized.<sup>2b,11</sup>

First, we synthesized a suitable folic acid derivative (**4**) incorporating a short PEG spacer and a primary amino function to facilitate conjugation with complex **2** via the formation of an amide bond (Scheme 1). Compound **4** was synthesized in two steps by reaction of the N-hydroxysuccinimidyl ester of folic acid and N-Boc-4,7,10-trioxa-1,13-tridecanediamine followed by acidic TFA treatment to remove the Boc group.<sup>11</sup> Then, complex **2** was attached to the amino-containing folate derivative by using a strong activator (HATU) in the presence of DIPEA in dry DMF for 2 h at RT under an Ar atmosphere and protected from light. The

expected Pt-folate conjugate (**3**) was obtained as a pale yellow solid (32 % yield) after purification by reversed-phase HPLC and lyophilization (Fig. S1, ESI†).



**Scheme 1.** Synthesis of Pt-folate conjugate (**3**).

Conjugate **3** was characterized by high-resolution ESI mass spectrometry,  $^1\text{H}$  and  $^{13}\text{C}$  NMR and UV-vis spectroscopy. An  $m/z$  value consistent with the calculated value of the charged species ( $[\text{M}-\text{H}]^-$  and  $[\text{M}-2\text{H}]^{2-}$ ) and with the expected isotopic mass distribution pattern of Pt was obtained (Fig. S2, ESI†). In addition, the assignment of the  $^1\text{H}$  NMR spectra of **3** in  $\text{DMSO}-d_6$  confirmed the covalent attachment of the Pt(IV) complex to folic acid. As shown in Fig. 2, the three expected signals of the pyridine ligands in the platinum complex were observed at 8.80, 8.27 and 7.82 ppm. In addition, all the diagnostic signals from the three components of folate backbone were clearly identified in the aromatic region of the  $^1\text{H}$  NMR spectra (Fig. 2): pterin (a singlet at 8.64 ppm corresponding to proton 7 of the heterocycle), *p*-aminobenzoate (two doublets at 7.64 and 6.63 ppm with  $J = 8.6$  Hz) and glutamate (the free  $\alpha$ -carboxyl group at 11.46 ppm as a broad singlet), together with three signals attributable to amide bonds in the Pt-folate conjugate. The UV-vis spectrum of conjugate **3** in PBS buffer was essentially the sum of those of the two fragments. On the one hand, both the  $\text{N}_3 \rightarrow \text{Pt(IV)}$  LMCT transition of the metal complex and the  $\pi-\pi^*$  electronic transitions of the pterin and *p*-aminobenzoate moieties of folic acid contribute to the broad absorption band around 290 nm (Fig. 2). On the other hand, the absorption band in the spectral range 300–400 nm can be assigned to  $n-\pi^*$  electronic transitions in folic acid.<sup>20</sup> As expected,  $^1\text{H}$  NMR analysis indicated that Pt-folate conjugate **3** was obtained as mixture of two constitutional isomers resulting from the attachment of the PEG linker in compound **4** to both the  $\alpha$  and  $\gamma$  carboxyl groups of folic acid, with the  $\gamma$ -carboxyl-linked derivative drawn in Scheme 1 being the major one (ca. 90%). These results are in good agreement with literature reports of other folate derivatives since the less hindered  $\gamma$  carboxyl group of folic acid reacts typically faster to give the  $\gamma$  regioisomer.<sup>6</sup> The mixture of  $\alpha$  and  $\gamma$  regioisomers of Pt-folate conjugate **3**, without further separation, was used in photoactivation and biological studies. In addition, it is

important to note that conjugate **3** was found to be completely stable after incubation for 24 h at 310 K in the dark in physiological-like conditions (Fig. S5, ESI†).

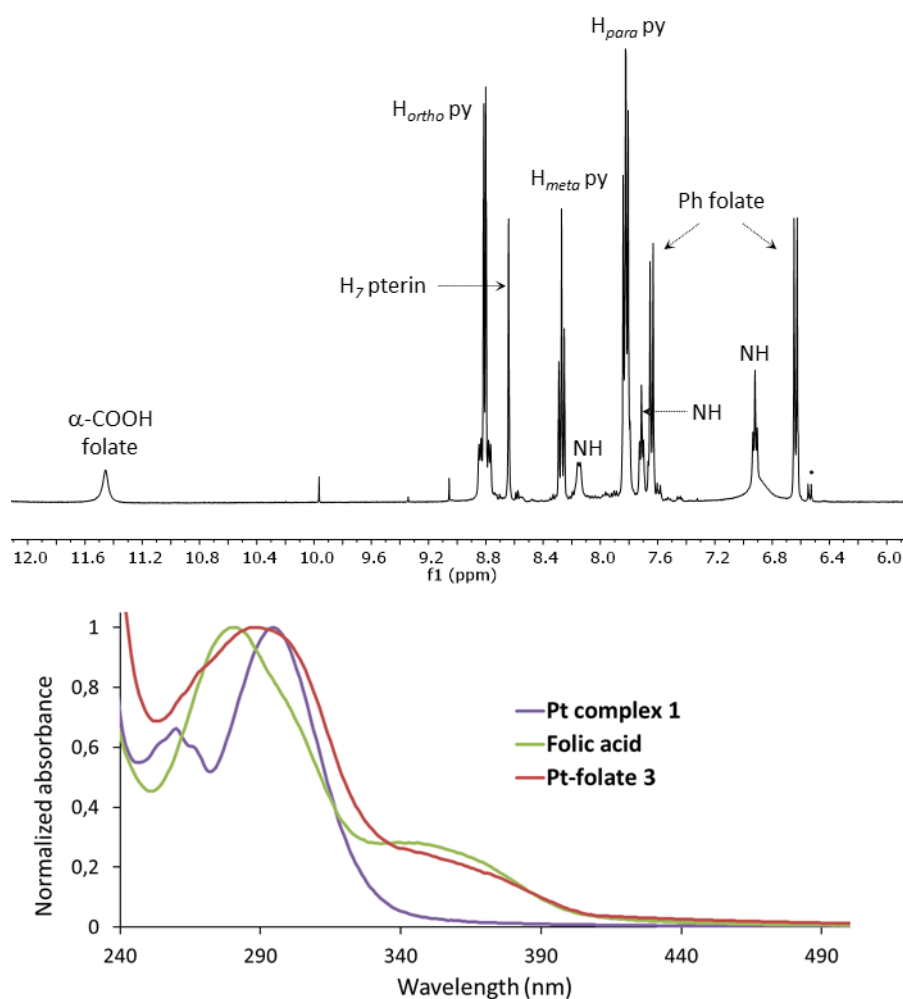


**Fig. 2** Characterization of Pt-folate conjugate **3**.  $^1\text{H}$  NMR spectra in  $\text{DMSO-}d_6$  showing the region between 6 and 12 ppm (top) and comparison of the UV-vis spectra of complex **1**, folic acid and conjugate **3** in PBS buffer at 298 K (bottom). \*This doublet corresponds to the *p*-aminobenzoate moiety of folic acid in the  $\alpha$  regioisomer of the conjugate.

Photoactivation of Pt-folate conjugate **3** was investigated in the presence of guanosine 5'-monophosphate (5'-GMP), since guanine nucleobases in DNA are known to be one of the main targets for Pt(II) photoproducts. Irradiation was performed with blue (420 nm) and green light (505 nm) in  $\text{H}_2\text{O}$  at 37 °C, and the course of the photoactivation process was monitored by reversed-phase HPLC-MS. As shown in Fig. 3, irradiation with blue light led to the complete disappearance of conjugate **3** and to the formation of the expected photolysis products (Scheme 2, pathway A) according to ESI-MS characterization: succinate-folate (**5**), photoreleased Pt(II) complex (**6**) and the Pt(II)-GMP adduct, *trans*-[Pt( $\text{N}_3$ )(5'-GMP)(py) $_2$ ] $^+$  (**7**) (GMP is considered neutral in all the formulae), which parallels the behavior previously

observed for the parent complex **1** and its peptide conjugates.<sup>15</sup> In addition, HPLC-MS analysis revealed the presence of compound **8** and several pterin derivatives, including 6-formylpterin (**9**), whose formation can be explained through the cleavage of the bond between the *p*-aminobenzoate-containing fragment and the pterin ring system in folate (Scheme 2, pathway B). To our surprise, cleavage of this bond also occurred at the level of the parent conjugate (Scheme 2, pathway C), which led to the formation of a Pt-folate conjugate lacking the pterin fragment (**10**), which was subsequently transformed into the expected photoproducts (**6-8**) due to photoreduction of the intact Pt(IV) complex. A minor non-photoactivatable Pt-folate conjugate lacking the pterin ring (**11**) was also identified in the crude mixture of photolysis products. Similar results were obtained upon irradiation with green light (Fig. S6, ESI†).

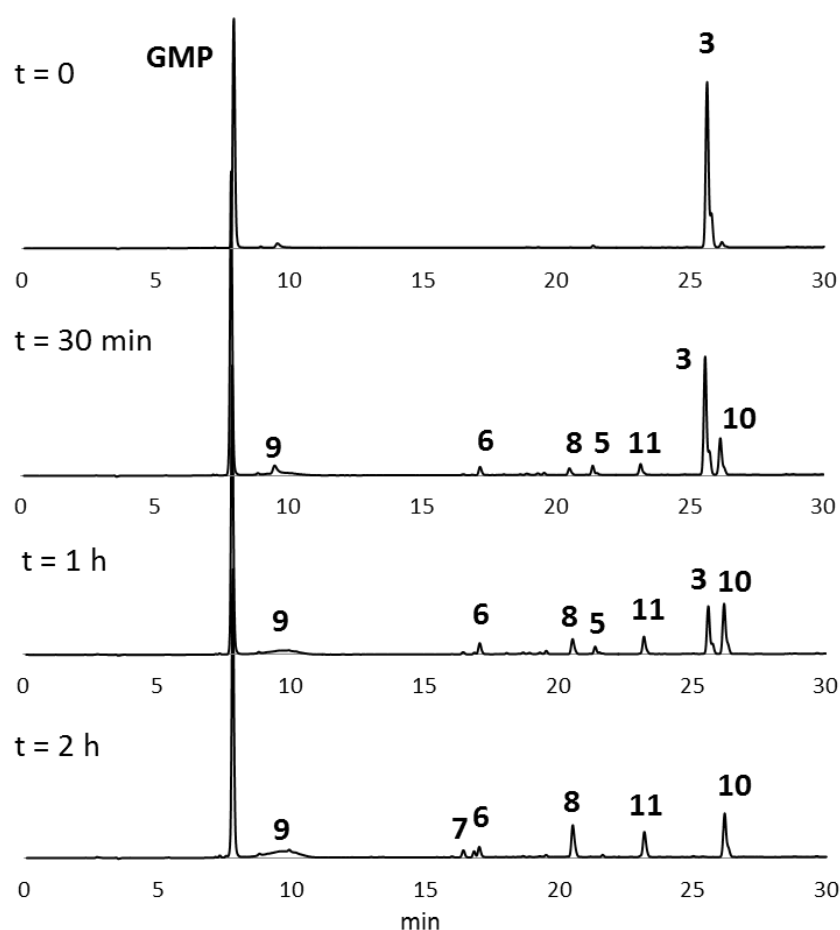
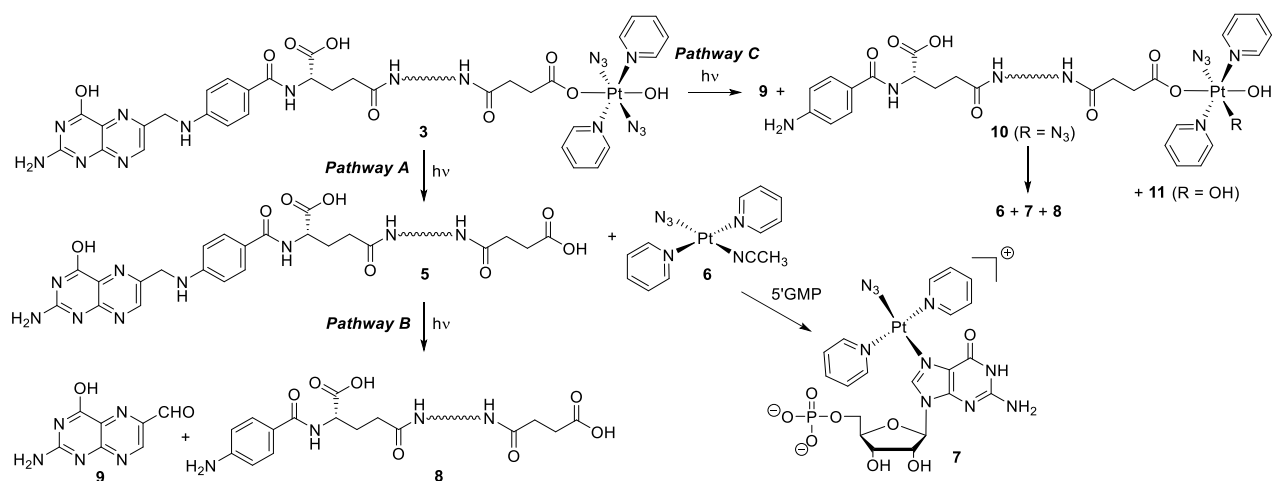


**Fig. 3** Reversed-phase HPLC-MS analysis of the photoactivation of Pt-folate conjugate **3** in the presence of 5'-GMP (2 mol equiv.) in H<sub>2</sub>O with blue light.

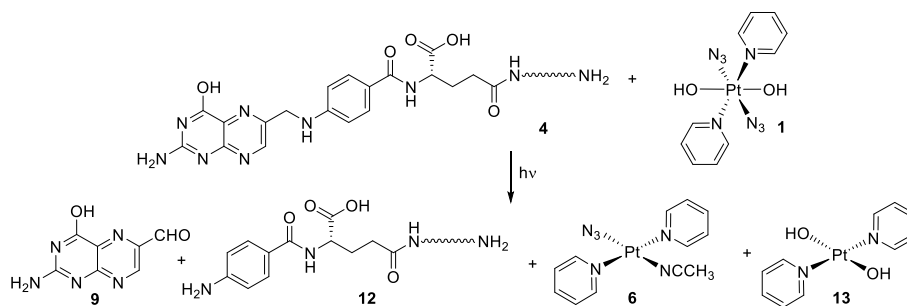


**Scheme 2.** Photoactivation pathways for Pt-folate conjugate **3**.

Since photodecomposition of folic acid into *p*-aminobenzoyl-L-glutamic acid and 6-formylpterin or 6-carboxypterin derivatives has been reported to occur upon irradiation with UV light,<sup>21</sup> we investigated the photostability of folate derivative **4** under the irradiation conditions. As shown in Fig S7 (ESI<sup>†</sup>), **4** was stable both after irradiation with blue (2 h, 37 °C) or green (1 h, 37 °C) light, which suggested the involvement of the Pt(IV) complex or its photoproducts in the photodegradation of folic acid. In order to confirm this hypothesis, we irradiated an equimolar mixture of **4** and complex **1**. Very interestingly, HPLC-MS analysis (Fig. S8, ESI<sup>†</sup>) revealed the presence of the *p*-aminobenzoate derivative **12** and 6-formylpterin **9** together with several Pt(II) photoproducts, with **6** and **13** being the main platinum species (Scheme 3). Further evidence of the photodecomposition of folic acid mediated by complex **1** was obtained by <sup>1</sup>H NMR spectroscopy. As shown in Fig. S9 (ESI<sup>†</sup>), green light irradiation of an equimolar mixture of folic acid and Pt(IV) complex **1** in DMSO-*d*<sub>6</sub>/D<sub>2</sub>O 8:2 (v/v) for 2 h at 37 °C led to the disappearance of the <sup>1</sup>H NMR peaks for the CH<sub>2</sub> group linking *p*-aminobenzoate and pterin moieties. In addition, the appearance of peaks around 9.9 ppm together with a shift of proton 7 of the pterin heterocycle to lower field (9.02 ppm vs. 8.61 ppm in free folic acid) confirmed the photodecomposition of folic acid in 6-formylpterin derivatives and in the *p*-aminobenzoyl-L-glutamic acid.

Overall, these experiments demonstrated the participation of the *trans*-diazido Pt(IV) complex on the photodegradation of folic acid, even when both compounds were not covalently attached. Oxidative attack of azidyl radicals produced by photodecomposition of complex **1** on the pterin heterocycle might trigger the cleavage of folic acid in a similar fashion as occurs with tryptophan amino acid and tryptophan-containing peptides.<sup>22</sup> Such unexpected results might be biologically relevant since pterin photoproducts generate

reactive oxygen species (ROS)<sup>21c</sup> and, consequently, the mechanism of action of Pt-folate conjugate **3** could involve photodynamic therapy (PDT) besides PACT.



**Scheme 3.** Photoactivation of an equimolar mixture of complex **1** and folate derivative **4**.

Having established the photoactivation properties of the Pt-folate conjugate **3**, we focused on investigating photocytotoxicity towards MCF-7 breast cancer cell line. Since conventional cell culture media contains a folic acid concentration much higher (*ca.* 2.2  $\mu\text{M}$ ) than that typically found in blood plasma (*ca.* 4.5-50 nM),<sup>23</sup> photocytotoxicity studies were carried out in folic acid-free DMEM to assess the effect of the folate vector on delivery of the metallodrug into MCF-7 cancer cells. The photocytotoxicity of conjugate **3** and of the parent Pt(IV) pro-drug (**1**) was determined upon irradiation with blue visible LED light ( $\lambda_{\text{irr}} = 465 \text{ nm}$ , 4.8  $\text{mW cm}^{-2}$ ). The dose-dependent inhibition of cell viability for the compounds towards MCF-7 cells, which was determined by the sulforhodamine B (SRB) colorimetric assay, and their phototoxic indices are summarized in Table 1. First, it is worth noting that both compounds are found non-toxic towards the MCF-7 cancer cell line in the dark with  $\text{IC}_{50}$  values  $>100 \mu\text{M}$ . However, irradiation with blue light led to a significant enhancement of the cytotoxicity in both cases, with the photocytotoxicity of Pt-folate conjugate ( $\text{IC}_{50} = 14.4 \mu\text{M}$ ) being greater than that of the parent Pt(IV) complex ( $\text{IC}_{50} = 32.4 \mu\text{M}$ ) with photocytotoxicity indices (PI) of  $>6.9$  and  $>3.0$ , respectively. Overall, these results indicate that the photocytotoxicity of the *trans*-diazido Pt(IV) pro-drug towards MCF-7 breast cancer cells can be significantly enhanced through conjugation with folic acid without compromising its dark toxicity.

**Table 1.** IC<sub>50</sub> values and photocytotoxicity indices (PI) for Pt-folate conjugate **3** and the parent Pt(IV) complex **1** in MCF-7 breast cancer cells after 1 h incubation, 1 h irradiation (blue 465 nm, 4.8 mW cm<sup>-2</sup>) and 24 h recovery.

		IC <sub>50</sub> (μM) <sup>a</sup>
Pt-folate conjugate <b>3</b>	Dark	> 100
	Irrad.	14.4 ± 1.0
	PI	> 6.9
Pt(IV) Complex <b>1</b>	Dark	> 100
	Irrad.	32.4 ± 3.3
	PI	> 3.0

<sup>a</sup> Data are from three independent experiments

Cellular accumulation of metal-based anticancer drugs usually plays an important role in their antiproliferative activity, especially when conjugated to targeting ligands whose receptors are overexpressed on the cell surface.<sup>24</sup> For this reason, we investigated platinum accumulation by MCF-7 cancer cells after exposure to 10 μM solutions of Pt-folate conjugate **3** and complex **1** for 1 h in the dark at 37 °C. Inductively-coupled plasma mass spectrometry (ICP-MS) was used to quantify the intracellular level of Pt in both cases (Table 2). Very interestingly, the cellular accumulation of Pt from conjugate **3** (5.8 ng per 10<sup>6</sup> cells) in MCF-7 cell line was about 9x higher than that of the parent complex **1** (0.67 ng per 10<sup>6</sup> cells), which is in good agreement with the higher photocytotoxicity of the conjugate. In order to obtain more insight into the participation of folate receptor in the cellular uptake of the conjugate, Pt accumulation studies were repeated at low temperature. As shown in Table 2, the incubation of MCF-7 cells with conjugate **3** at 4 °C led to a reduction in the Pt accumulation (ca. 33 %). Competitive studies with folic acid further confirmed the involvement of folate receptor in the internalization of the Pt-folate conjugate in breast cancer cells, which have been reported to exhibit medium folate receptor expression on their surface.<sup>25</sup> Indeed, pre-treatment of MCF-7 cells with folic acid (100 mol equiv.) led to a slight reduction in Pt accumulation from **3**. Overall, these results suggest the participation of the folate receptor in the cellular uptake of Pt-folate conjugate in MCF-7 cells and that it enters the cells through an energy-dependent pathway and not only by passive diffusion.

**Table 2.** Cell accumulation of Pt (ng per 10<sup>6</sup> cells) in MCF-7 cancer cells after exposure to Pt-folate conjugate **3** and the parent Pt(IV) complex **1** (10  $\mu$ M, 1 h, in the dark).

Compound	Temperature	Platinum accumulation (ng per 10 <sup>6</sup> cells) <sup>a</sup>
Pt-folate conjugate <b>3</b>	4°C	3.9 $\pm$ 0.6
	37°C	5.8 $\pm$ 0.4 <sup>***</sup>
Pt-folate+100 eq folate	37°C	5.5 $\pm$ 0.7 <sup>**</sup>
Complex <b>1</b>	37°C	0.67 $\pm$ 0.12 <sup>*</sup>

<sup>a</sup> All data were determined from triplicate samples and compared with values obtained for untreated cells using a two-tail *t*-test with unequal variances. \**p* < 0.05, \*\**p* < 0.01, \*\*\**p* < 0.005.

In summary, we have synthesized and characterized a novel conjugate between a photoactivatable *trans*-diazido Pt(IV) pro-drug and folic acid with the aim of generating folate-receptor targeted anticancer metallodrugs operating with a novel mechanism of action. Photoactivation of the Pt-folate conjugate with visible light confirmed the generation of cytotoxic Pt(II) species capable of binding to guanine nucleobases. In addition, photoreduction of the Pt(IV) complex was accompanied by the photodecomposition of the folate vector into a *p*-aminobenzoate-containing fragment and several pterin derivatives, including 6-formylpterin, a process that might be triggered by azidyl radicals produced during the photoactivation of the Pt(IV) pro-drug. Besides exhibiting high dark stability under physiological-like relevant conditions, the Pt-folate conjugate was found *ca.* 2x photocytotoxic towards MCF-7 breast cancer cell line than its parent Pt(IV) complex. The higher photocytotoxicity of the conjugate (PI >6.9) compared with the parent Pt(IV) pro-drug (PI >3.0) might be attributable both to a higher cellular accumulation and to the generation of several cytotoxic species, including Pt(II) photoproducts and pterin derivatives which are known to generate ROS. This work suggests for the first time that folic acid conjugation to photoactivatable metallodrugs could be exploited to improve selectivity towards cancer cells overexpressing folate receptor as well as to attack them by combining PACT and PDT. Work is in progress to investigate the contribution of photoreleased pterin derivatives to the photocytotoxicity of such Pt-folate conjugates.

### Acknowledgements

This work was supported by funds from the Spanish Government (MCIU/AEI/FEDER, UE; grants CTQ2017-84779-R) and the Generalitat de Catalunya (2017 DI 072), EPSRC (grant no EP/P030572/1), a University of Warwick Chancellor's Scholarship (for H.S.) and Anglo American Platinum. We acknowledge helpful assistance of Dr. Francisco Cárdenas (NMR)

and Dr. Irene Fernández and Laura Ortiz (MS) from CCiTUB, and technical assistance at the University of Warwick from Drs Lijiang Song and Ivan Prokes. A.G. and A.R. were recipient fellows of the University of Barcelona.

## References

- 1 a) L. Xu, Q. Bai, X. Zhang and H. Yang, *J. Controlled Release*, 2017, **252**, 73; b) M. Scaranti, E. Cojocar, S. Banerjee and U. Banerji, *Nat. Rev. Clin. Oncol.*, 2020, **17**, 349.
- 2 a) P. S. Low and S. A. Kularatne, *Curr. Opin. Chem. Biol.*, 2009, **13**, 256; b) W. Xia and P. S. Low, *J. Med. Chem.*, 2010, **53**, 6811; c) L. Teng, J. Xie, L. Teng and R. J. Lee, *Expert Opin. Drug. Deliv.*, 2012, **9**, 901; d) M. Fernández, F. Javaid and V. Chudasama, *Chem. Sci.*, 2018, **9**, 790.
- 3 A. Guaragna, A. Chiaviello, C. Paoletta, D. D'Alonzo, G. Palumbo and G. Palumbo, *Bioconjugate Chem.*, 2012, **23**, 84.
- 4 a) J. W. Lee, J. Y. Lu, P. S. Low and P. L. Fuchs, *Bioorg. Med. Chem.*, 2002, **10**, 2397; b) J. D. Seitz, J. G. Vineberg, E. Herlihy, B. Park, E. Melief and I. Ojima, *Bioorg. Med. Chem.*, 2015, **23**, 2187.
- 5 J. A. Reddy, E. Westrick, I. Vlahov, S. J. Howard, H. K. Santhapuram and C. P. Leamon, *Cancer Chemother. Pharmacol.*, 2006, **58**, 229.
- 6 M.-R. Ke, S.-L. Yeung, D. K. P. Ng, W.-P. Fong and P.-C. Lo, *J. Med. Chem.*, 2013, **56**, 8475.
- 7 C. P. Leamon, I. R. Vlahov, J. A. Reddy, M. Vetzal, H. K. Santhapuram, F. You, A. Bloomfield, R. Dorton, M. Nelson, P. Kleindl, J. F. Vaughn and E. Westrick, *Bioconjugate Chem.*, 2014, **25**, 560.
- 8 P. Mc Carron, A. Crowley, D. O'Shea, M. McCann, O. Howe, M. Hunt and M. Devereux, *Curr. Med. Chem.*, 2018, **25**, 2675.
- 9 a) R. G. Kenny and C. J. Marmion, *Chem. Rev.*, 2019, **119**, 1058; b) E. Boros, P. J. Dyson and G. Gasser, *Chem*, 2020, **6**, 41; c) A. Khoury, K. M. Deo and J. R. Aldrich-Wright, *J. Inorg. Biochem.*, 2020, **207**, 111070.
- 10 O. Aronov, A. T. Horowitz, A. Gabizon and D. Gibson, *Bioconjugate Chem.*, 2003, **14**, 563.
- 11 S. Dhar, Z. Liu, J. Thomale, H. Dai and S. J. Lippard, *J. Am. Chem. Soc.*, 2008, **130**, 11467.
- 12 a) N. J. Farrer, L. Salassa and P. J. Sadler, *Dalton Trans.*, 2009, **48**, 10690; b) C. Imberti, P. Zhang, H. Huang and P. J. Sadler, *Angew. Chem. Int. Ed.*, 2020, **59**, 61.
- 13 a) N. J. Farrer, J. A. Woods, L. Salassa, Y. Zhao, K. S. Robinson, G. Clarkson, F. S. Mackay and P. J. Sadler, *Angew. Chem. Int. Ed.*, 2010, **49**, 8905; b) H. Shin, C. Imberti and P. J. Sadler, *Inorg. Chem. Front.*, 2019, **6**, 1623.

14 a) T. C. Johnstone, K. Suntharalingam and S. J. Lippard, *Chem. Rev.*, 2016, **116**, 3436; b) Y. Yuan, R. T. K. Kwok, B. Tang and B. Liu, *J. Am. Chem. Soc.*, 2014, **136**, 2546; c) Y. Zheng, K. Suntharalingam, T. C. Johnstone, H. Yoo, W. Lin, J. G. Brooks and S. J. Lippard, *J. Am. Chem. Soc.*, 2014, **136**, 8790; d) S. G. Awuah, Y. Zheng, P. M. Bruno, M. T. Hemann and S. J. Lippard, *J. Am. Chem. Soc.*, 2015, **137**, 14854; e) E. Petruzzella, J. P. Braude, J. R. Aldrich-Wright, V. Gandin and D. Gibson, *Angew. Chem. Int. Ed.*, 2017, **56**, 11539.

15 a) A. Gandioso, E. Shaili, A. Massaguer, G. Artigas, A. González-Cantó, J. A. Woods, P. J. Sadler and V. Marchán, *Chem. Commun.*, 2015, **51**, 9169; b) H. Shi, Q. Wang, V. Venkatesh, G. Feng, L. S. Young, I. Romero-Canelón, M. Zeng and P. J. Sadler, *Dalton Trans.*, 2019, **48**, 8560.

16 Y. Min, J. Li, F. Liu, E. K. L. Yeow and B. Xing, *Angew. Chem. Int. Ed.*, 2014, **53**, 1012.

17 V. Venkatesh, N. K. Mishra, I. Romero-Canelón, R. R. Vernooij, H. Shi, J. P. C. Coverdale, A. Habtemariam, S. Verma and P. J. Sadler, *J. Am. Chem. Soc.*, 2017, **139**, 5656.

18 D. Zhou, J. Guo, G. B. Kim, J. Li, X. Chen, J. Yang and Y. Huang, *Adv. Healthcare Mater.*, 2016, **5**, 2493.

19 F. Barragán, P. López-Senín, L. Salassa, S. Betanzos-Lara, A. Habtemariam, V. Moreno, P. J. Sadler and V. Marchán, *J. Am. Chem. Soc.*, 2011, **133**, 14098.

20 M. Baibarac, I. Smaranda, A. Nila and C. Serbschi, *Sci. Rep.*, 2019, **9**:14278.

21 a) M. K. Off, A. E. Steindal, A. C. Porojnicu, A. Juzeniene, A. Vorobey, A. Johnsson and J. Moan, *J. Photochem. Photobiol. B.*, 2005, **80**, 47; b) C. B. Martin, D. Walker and M. Soniat, *J. Photochem. Photobiol. A.*, 2009, **208**, 1; c) A. Juzeniene, M. Grigalavicius, L. W. Ma and M. Juraleviciute, *J. Photochem. Photobiol. B.*, 2016, **155**, 116.

22 a) J. S. Butler, J. A. Woods, N. J. Farrer, M. E. Newton and P. J. Sadler, *J. Am. Chem. Soc.*, 2012, **134**, 16508; b) C. Vallotto, E. Shaili, H. Shi, J. S. Butler, C. J. Wedge, M. E. Newton and P. J. Sadler, *Chem. Commun.*, 2018, **54**, 13845.

23 Y. Cao and J. Yang, *Bioconjugate Chem.*, 2014, **25**, 873.

24 a) F. Barragán, V. Moreno and V. Marchán, *Chem. Commun.*, 2009, 4705; b) F. Barragán, D. Carrion-Salip, I. Gómez-Pinto, A. González-Cantó, P. J. Sadler, R. de Llorens, V. Moreno, C. González, A. Massaguer and V. Marchán, *Bioconjugate Chem.*, 2012, **23**, 1838; c) A. Massaguer, A. González-Cantó, E. Escribano, S. Barrabes, G. Artigas, V. Moreno and V. Marchán, *Dalton Trans.*, 2015, **44**, 202.

25 S. K. Bhunia, A. R. Maity, S. Nandi, D. Stepensky and R. Jelinek, *ChemBioChem*, 2016, **17**, 614.